BEACON SATELLITE STUDIES OF SMALL SCALE IONOSPHERIC INHOMOGENEITIES

by

J. P. McClure

and

G. W. Swenson, Jr.

May, 1964

Sponsored by

NsG 24-59

National Aeronautics and Space Administration

Washington 25, D. C.

Department of Electrical Engineering
Engineering Experiment Station
University of Illinois
Urbana, Illinois

BEACON SATELLITE STUDIES OF SMALL SCALE IONOSPHERIC INHOMOGENEITIES

by

J. P. McClure

and

G. W. Swenson, Jr.

May, 1964

Sponsored by

NsG 24-59

National Aeronautics and Space Administration

Washington 25, D. C.

Department of Electrical Engineering
Engineering Experiment Station
University of Illinois
Urbana, Illinois

Abstract

N64-22421 over

Scintillation of radio signals from artificial earth satellites has been studied with a network of spaced receivers. The height of the irregularities responsible for scintillation was measured by the cross-correlation method for 130 satellite passages. Theoretical calculations show that the cross-correlation method used gives the average irregularity height when irregularities are uniformly distributed over a finite height range. The irregularity height measurements were made continuously for all scintillation observed sufficiently close to the receiver network. The irregularity height in the F-region was found to be fairly constant for about 2/3 of the passages examined, and to be more or less variable about 1/3 of the time. The average height gradient for individual cases where the irregularity height is not constant was near zero. Increases in irregularity height to the north and to the south occurred with approximately equal probability. Height gradients were seldom uniform for more than 50-100 km. The average height of all F-region irregularities increased to the north. This was not due to uniform layers of irregularities gently sloping upward to the north, but to irregularity patches, large and small, being higher, on the average, in the north. The heights of the irregularities in the E-region below 130 km were constant, and had no gradients, unlike the irregularities in the F-region.

Sufficient data were obtained to determine the diurnal variation of the irregularity height distribution. The data show conclusively that most daytime scintillation originates in the E-region near 110 km height,

22421

and that most nighttime scintillation originates in the F-region at heights between 300 and 400 km. When E or F-region irregularities were observed near an ionosonde, they were nearly always accompanied by sporadic-E or spread-F echoes on the ionogram. The F-region irregularity height distribution was considerably broader after midnight than before midnight. There were not enough data to tell whether or not there was any seasonal variation of the irregularity height distribution.

Theoretical calculations resulted in a cross-correlation function describing the changes in the signal strength pattern on the ground which are observed in spaced receiver experiments. A concise expression was obtained for the cross-correlation as a function of the thickness and average height of a uniform slab of irregularities, the size of the irregularities, and the receiver spacing. After the cross-correlation has fallen to 0.5, it is approximately an inverse function of distance. The calculations are based on work in scattering theory by Yeh. A formula derived from the diffraction theory by James can be obtained as a special case of the cross-correlation function developed here. The cross-correlation function is applied to experimental data and the thickness of the layer of irregularities is found. For F-region scintillation the thickness varied from 50 km to over 300 km, with an average of approximately 120 km. Author

Acknowledgement

The authors wish to thank Dr. K. C. Yeh for much valuable advice during this work. The ionosonde data were supplied by the University of Illinois Radiolocation Research Laboratory and the U. S. Army Signal Corps. Satellite orbital data were supplied by the Applied Physics Laboratory of Johns Hopkins University and by the Goddard Space Flight Center. The cooperation of the Applied Physics Laboratory in keeping Transit IV-A turned on in the 54-324 mc mode is gratefully acknowledged. This work was sponsored by the National Aeronautics and Space Administration under Grant NASA NsG 24-59.

Table of Contents

Chapter I. Introduction and Historical Survey

1. The Cause of Scintillation

Radio signals from beacon satellites have been used to study the small-scale inhomogeneities in the electron density of the ionosphere. These irregularities, when present, cause scattering of radio signals propagated through them, resulting in irregular patterns of signal strength on the ground. Radio scintillation is a random time variation of the amplitude and phase of a radio signal which has propagated through a region of ionospheric inhomogeneities. Roughly speaking, shadows of the ionospheric inhomogeneities are cast on the earth, and give rise to the scintillation.

Radio scintillation is analogous to visual star scintillation or twinkling. Examples of both kinds of scintillation are shown below. Figure 1 shows an example of optical star scintillation observed with a telescope and a photocell. The ordinate is proportional to the photocell current or light intensity. Figure 2 shows an example of satellite radio scintillation. The ordinate is proportional to the receiver AGC voltage or logarithmic radio signal intensity.

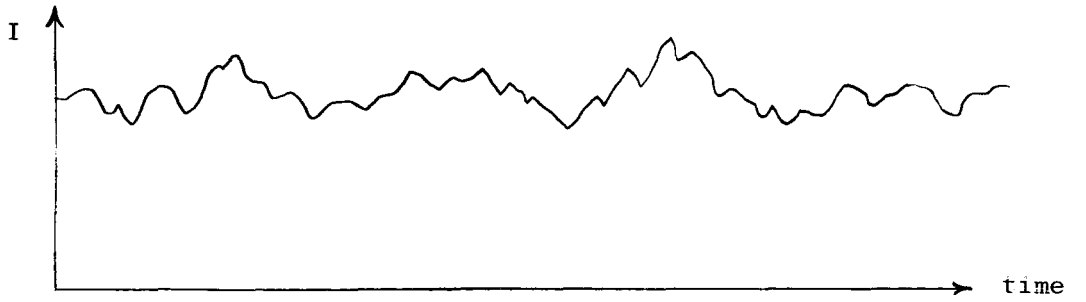

Figure 1. Optical Star Scintillation

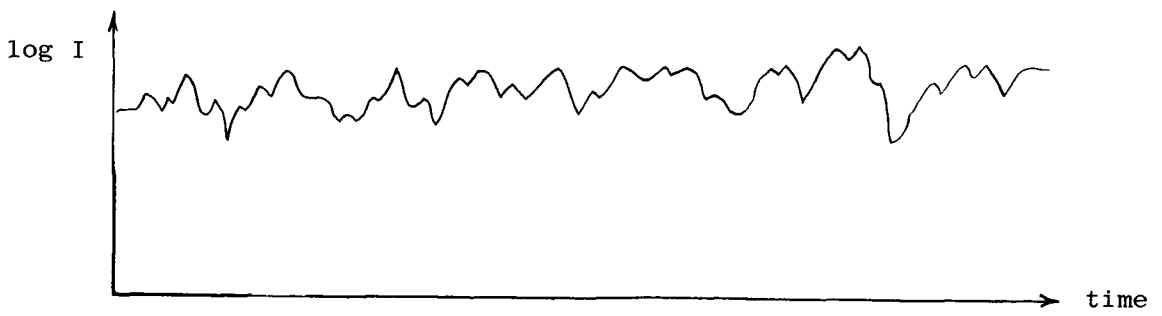

Figure 2. Radio Satellite Scintillation

Figures 1 and 2 display similar, random variations of signal intensity as a function of time. In both cases the variations are caused by irregularities in the dielectric constant of the atmosphere. For light waves, the dielectric constant is highest where the air density is greatest, i.e. in the lowest few kilometers of the atmosphere. Air density irregularities are always present in the troposphere due to turbulence and it is these irregularities which cause optical scintillation. However, at radio wavelengths greater than about 30 cm the dielectric constant of the ionosphere becomes much larger than the dielectric constant of the troposphere. Therefore it is ionospheric irregularities which cause radio scintillation.

We shall trace the evolution of ideas about scintillation in order to provide historical background. We now know it is caused by irregularities in the earth's atmosphere. At first it was believed that the twinkling of stars was caused by rapid variations in the brightness and position of the stars themselves, which were imagined to be like distant flickering candles. Some time later, Aristotle wrote about twinkling, rejecting on purely intellectual grounds the idea that stars

could be anything like flickering candles. Instead, he thought they were very much like the sun and explained twinkling on the basis of the "great distance to the sphere of the stars" and "the weakness of our vision." Aristotle's explanation was still being advocated as recently as 1950 by a London optometrist [Hartridge, 1950]. His experiments showed that a faint but steady light does appear to twinkle due to physiological reasons, just as Aristotle had believed. However, observed evidence, such as photoelectric records like Figure 1, cannot be explained on this basis.

When the appropriate data are available, the correct interpretation of optical scintillation becomes clear. The "scintillation index," which is defined as the root mean square of the signal fluctuations divided by the mean signal intensity, increases as a star approaches the horizon. This indicates that the fluctuations are not due to variations in the brightness of the star, but are introduced in the earth's atmoshpere. The fluctuations could result from the motion of a light pattern across the telescope, from changes in an unmoving light pattern, or from a combination of these two processes. This ambiguity may be resolved in an experiment where two telescopes are placed about 10 cm apart. The light intensity records are well correlated, differing mainly by a time shift. As the telescope spacing is increased, the time shift is increased, but the cross-correlation of the records is reduced. These data are consistent with the effect that would be expected from a changing random pattern of light moving past the telescopes.

Thus the evidence indicates that optical scintillation is the result of a light pattern which moves past the eye. This pattern might look

like the light pattern formed on the bottom of a swimming pool. The structure and motion of the pool pattern is determined by the structure and motion of the irregularities on the surface of the pool. In a similar manner the structure and motion of an optical scintillation pattern is related to the atmospheric irregularities which create it.

Another example, a favorite of J. A. Ratcliffe, a pioneer in ionosphere studies, is the effect of heat waves rising from a hot surface on a summer day. The air density in heat waves is very irregular because of the turbulent mixing of warm and cold air. Distant objects viewed through the heat waves appear to flicker and waver in an effect analogous to scintillation.

2. Radio Star Scintillation Results

Radio signals from the "stars" were discovered by Karl Jansky in 1932. (Note: most astronomical radio sources are not, strictly speaking, stars.) In 1946, it was discovered that the intensity of the radio signal received from the strong source in Cygnus was variable [Hey, Parsons and Phillips, 1946]. The development of the correct explanation of this phenomenon was closely parallel with the development of the explanation of optical star scintillation. Again, it was first believed that the variations were due to fluctuations in the source itself [Hey et al., 1946]. Again, later experimental evidence proved this explanation wrong. As with light, it is not possible to interpret completely a single time versus signal strength record of scintillation (example shown in Figure 2). The variations could be caused by the motion of a fixed pattern of radio signal

strength past the antenna, by changes in an unmoving pattern of signal strength or both. To study scintillation-producing irregularities in detail it is necessary to study the distribution of signal strength over the ground, its motions and its changes. To do this, data from several points on the ground are necessary. Using a pair of receivers spaced 3.9 km apart, recordings of the signals from Cygnus were found to be similar (50 to 95 percent correlated), but for a spacing of 20 km, "No detailed correlation could be found" [Smith, 1950; Little and Lovell, 1950]. Thus it was first revealed that radio star scintillation must be introduced somewhere in the earth's atmosphere.

Ryle and Hewish [1950] separated a pair of receivers by 1 km in the east-west direction. They observed well-correlated records with time delays corresponding to drift velocities in the order of 100 to 200 meters per second. The time delay and the average number of maxima per minute indicated the distance between maxima in the pattern was approximately constant and about 5 km in magnitude. It was concluded that changes in the fluctuation rate of the scintillation were mainly caused by changes in the drift rate of the irregularities.

Little and Maxwell [1951] used a pair of receivers separated by approximately 4 km in the north-south direction and found approximately 50 percent correlation between the outputs. They also observed that the drift velocities of the irregularity pattern in the north-south direction were much less than the drift velocities in the east-west direction reported by Ryle and Hewish.

Spencer [1955] made a fundamental discovery by setting up three receivers in a triangular array. He found that the irregularities in the radio signal strength pattern on the ground were elongated by at least 5:1. The direction of elongation was always within 5 degrees of the ground projection of a line of force of the earth's magnetic field, and the average distance between maxima of the irregularities on the ground was about 3 km in the direction of the shortest dimension. From this evidence, he concluded that the ionospheric irregularities responsible for scintillation are also elongated by about 5:1 and are aligned with the earth's magnetic field.

In Australia, Wild and Roberts [1956] reported that measurements of radio star intensity versus frequency and time seemed to imply that many of the fluctuations observed were due to a sort of focusing by single, lens-like irregularities. Concurrent spaced receiver studies of the size and shape of nighttime irregularities agreed with Spencer's results. They also observed daytime irregularities not reported by Spencer. This discrepancy has been attributed to sporadic-E and to the differences in elevation of the source as viewed from England and Australia [Booker, 1958].

Recently, similar spectral observations have been made at Boulder by Warwick [1964]. He finds that about 10 percent of the scintillation observed can be the result of the focusing effect of single, wavelike irregularities, confirming the results of Wild and Roberts.

In summary, spaced receiver outputs are similar, except for time shifts. Larger receiver spacing increases the time shift and decreases

the correlation, but so slowly that the output of a single receiver may be assumed to be caused by drift of an unchanging pattern. If receivers are spaced far enough apart in the direction of pattern drift, correlation is eventually reduced to zero. We conclude from spaced receiver observations that field-aligned irregularities in ionospheric electron density cause the irregular pattern of radio star signal strength on the ground and that these irregularities are highly elongated and drift at 100 to 200 meters per second in temperate latitudes.

We shall now review some other basic aspects of radio star scintillation. The diurnal variation of average scintillation index has a maximum near midnight. Good correlation between the occurrence of scintillation and spread-F on ionograms was observed by Ryle and Hewish [1950] and by Little and Maxwell [1951]. In contrast, correlation of scintillation with sporadic-E, but not with spread-F, was observed by Bolton, Slee and Stanley [1951] in Australia, and Dueño [1955] at Cornell University. The accepted explanation of this apparent disagreement is that the correlation with spread-F will occur for nighttime scintillation observed near the zenith, while the correlation with sporadic-E will occur for daytime scintillation observed at low elevation angles.

The height of the irregularities was not well known. In his review paper, Booker [1958] stated that the available data were adequate only to establish that nighttime scintillation is caused mainly by F-region irregularities. There is no really accurate way of measuring the height of irregularities using radio stars. Briggs [1958] had a simple method that produced some approximate results. He postulated that the correlation

of radio star scintillation with spread-F at a remote ionosonde would depend on the height assumed for the scintillation irregularities. Briggs found that for heights of 250-300 km, the correlation between the two phenomena was maximum.

Earlier, Hewish [1952] had attempted to measure the irregularity height through a comparison of phase and amplitude scintillation. It is theoretically possible to do so, but in actual practice it is very hard to get accurate results because it is difficult to measure phase scintillation with sufficient precision. The theoretical work of Hewish [1952] was based on the diffraction theory. Similar results were obtained by Yeh [1962] on the basis of scattering theory. Hewish made thirteen separate measurements, resulting in a wide spread in the heights obtained (5:1). He gave 400 km as the average height of irregularities. All the heights obtained were in the F-region. For lack of accuracy, this method has not been used since.

An excellent review of radio star scintillation, including additional results not pertinent here, is given by Booker [1958].

3. Satellite Scintillation Results

On October 5, 1957, the first artificial earth satellite, Sputnik I, was launched. The 20 mc beacon transmitter on board was observed to scintillate on at least part of nearly every pass recorded at the University of Illinois, especially when the satellite was in the north. Since satellites cover a large part of the sky on every pass, and since there are two close passes per day for each satellite whose orbital plane has a sufficiently high inclination with the earth's equator, beacon satellites

give a large amount of scintillation data. Extensive studies of the diurnal, seasonal, and latitude variation of scintillation have been made using them.

The diurnal variation of average scintillation index shows a maximum near midnight. The latitude variation is summarized by Yeh, Swenson and McClure [1963] and by Yeh and Swenson [1964]. The results show that the average scintillation index increases abruptly with latitude at the time of the sunspot maximum, and that seasonal, sunspot number and solar cycle variations influence the latitude variation of scintillation. In contrast Lawrence and Martin [1964] and Yeh and Swenson [1964] have found evidence of a slight increase of scintillation activity to the south in 1962.

The variation of spread-F occurrence probability behaves in the same way. The diurnal variation also shows a maximum near midnight. Shimazaki [1959] has summarized the latitude variations. Near the sunspot maximum the occurrence of spread-F increases sharply to the north at the latitude of the University of Illinois, 50° north geomagnetic latitude. There is very little spread-F occurring to the south of this parallel, but there is a steep rise in spread-F activity to the north of it. His data for the sunspot minimum show there is very little latitude variation of spread-F occurrence. There appears to be a slight increase in spread-F activity to the south at 50° geomagnetic latitude, during the sunspot minimum, in agreement with the satellite data above.

As mentioned before, radio star scintillation studies cannot accurately locate the height of the scintillation-producing irregularities. Artificial

earth satellites offer several good ways of measuring irregularity height. The easiest method is to observe the variation of the average scintillation index with satellite height. Using this method, it has been reported that most of the irregularities are within the following height ranges: 200 to 400 km at Baker Lake, Northwest Territories [Swenson and Yeh, 1961]; 270 to 325 km at Cambridge, England [Kent, 1959]; 250 to 650 km at College, Alaska [Basler and DeWitt, 1962]. However, these ranges are based on a large number of passes, and this method does not permit the measurement of the exact height on a particular pass.

Since the satellite velocity is very much greater than the drift velocity of the ionospheric irregularities, the ground velocity of the pattern is determined only by the satellite velocity, the satellite height, and the irregularity height (equation 1). Therefore, the exact irregularity height at a given time may be measured by using spaced receivers to determine the velocity of the irregularity pattern on the ground. The ground velocity may be determined by two methods.

The first and simplest method is called the "transition edge" method. Transitions from scintillation to Faraday fading or vice versa are often very abrupt, often taking one second or less, indicating that the ray to the satellite has just passed the edge of a region of irregularities (see Figure 3 below). By spacing receivers in the direction of satellite motion and observing the difference in the transition times, the height of the edge of the irregularity region is easily found. This method was first used at College, Alaska [Parthasarathy, Basler and DeWitt, 1959], revealing that irregularities exist at heights from 100 to 1000 km. Later, 23 heights

varying from 145 to 1000 km were observed by this method, also at College, Alaska [Basler and DeWitt, 1962]. A set of six "transition edge" measurements yielding heights from 320 to 430 km were made at the University of Illinois [Yeh, Swenson and McClure, 1963].

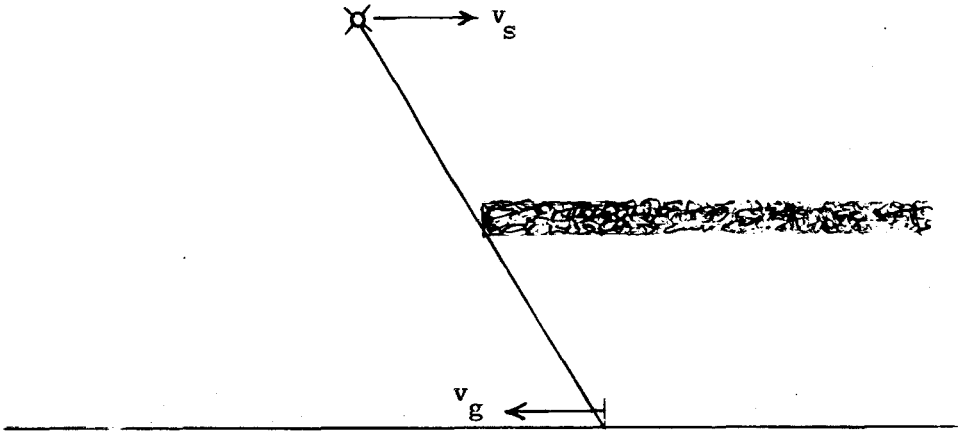

Figure 3. Geometry of the "Transition Edge" Method of Finding Ionospheric Irregularity Height

The second method of measuring the pattern velocity on the ground is to cross-correlate the output of two spaced receivers. Details of the use of the cross-correlation method are discussed in Chapter III. Briefly, the geometry of measuring the height by this method is the same as that of the transition edge method. The difference in methods is that rather than measuring the ground velocity of the transition edge, we measure the cross-correlation time delay of two relatively closely-spaced receivers and thus determine the ground velocity of the irregularity pattern itself. Many investigators have used this method, but the total number of measurements made has been too small to draw any detailed conclusions. Two measurements of 340 and 365 km were made by Frihagen and Tröim [1960] in Norway. Hook

and Owren [1962] found irregularities from 100 to 275 km (the height of the satellite used) for three passes recorded at College, Alaska. Thirteen measurements were made at Pennsylvania State University [DeBarber, 1963], yielding heights of 330 to 540 km. Fourteen measurements between 270 and 390 km were made at Gorki State University by Yerukimov [1962]. Forty-eight measurements varying from 100 to 1000 km were made by Liszka [1963b] in Sweden. Apparently, the largest number of such measurements was made by Jespersen and Kamas [1963] at Boulder. They do not state exactly how many measurements were made, but it appears that they computed the irregularity height at about 60 to 80 discrete points on some 20 usable spaced receiver records. They reported heights ranging from 200 to 700 km for nighttime passages. Most of the heights were between 250 and 400 km, and the average height was 325 km. A summary of ionospheric irregularity height measurements has been made by Chivers [1963].

This report extends the previous work by giving the results of continuous height measurements during the entire satellite passage rather than measurements at one or more discrete satellite positions. In Chapter III the statistical variations of the irregularity heights of a large number of passages (130) are presented.

Equation (1) is geometrically valid for measuring the height of thin irregularity layers, but has been used for thick layers. It is known that ionospheric irregularities are sometimes spread over considerable height range. Since irregularities at different heights should produce irregularity patterns on the ground which move at different velocities, it is not certain that Equation (1) applies for the cross-correlation

method under all conditions. Certainly some kind of "effective height" will be obtained, but its meaning in the "thick layer" case has not been examined heretofore. It is shown in Chapter IV of this report that if we assume a uniform slab of irregularities, the height obtained by the cross correlation method is the average height of the irregularities in the slab. This is a step toward clarifying the meaning of cross-correlation height measurements.

In addition to clarifying height measurements, the theoretical calculations in Chapter IV indicate that cross-correlation spaced receiver experiments can determine the thickness of the region of ionospheric irregularities responsible for satellite scintillation, provided that it is assumed that the irregularities are weak, so that only single scattering is important (Born approximation). A particular geometry is chosen (see Figure 9), where receivers are separated by a distance x in the direction of satellite motion, and the cross-correlation is computed. It will be shown that the cross-correlation of the outputs of spaced receivers is a maximum for this geometry, and that the magnitude of this function decreases monotonically with receiver spacing x and irregularity region thickness b. When the maximum cross-correlation between spaced receiver outputs is 0.5 or less, it decreases inversely with x and b (see Equation (30)). Thus spaced receiver experiments can be used to determine the thickness b.

This concept was previously exploited by James [1962], who derived a formula relating irregularity region thickness to satellite scintillation pattern change. His formula was derived from the diffraction theory. It is shown in Chapter IV of this report that James' formula can be obtained as a special case of the cross-correlation function derived there.

James' formula was applied by Jespersen and Kamas [1963]. They found irregularity region thicknesses from 120 to 470 km. Thickness measurements made using the cross-correlation function are presented in Chapter IV and compared to the above measurements and to thickness measurements made by other methods.

Chapter II. Experimental Procedure

1. Spaced-Receiver Data Acquisition Techniques

A mobile satellite receiving station was set up in a van having an auxiliary generator to power the equipment when no external power was available. An FM-FM telemetry link transmitted the remote satellite signal strength information to the base station for recording. Tone signaling equipment in the van made it possible to turn on the remote station VHF telemetry transmitter from the base station. Receiver spacings of 2 to 35 km were used with this equipment.

Ultimately, leased phone lines replaced the VHF telemetry link, and battery operated transistorized receivers replaced the AC operated frequency converters and military communication-type receivers. It was found desirable to have more than one spaced receiver, and in the final six months of the experiment, four receiver locations were used. Conventional turnstile antennas and conventional communication-type receivers having a 3 or 4 kc bandwidth were used throughout the study.

2. Satellite Orbital Characteristics

The satellite used in this study was Transit IV-A. It had an inclination of 66.8^{o} and a height of 900-1000 km above the earth and carried a 54 mc beacon transmitter. Table 1 gives the various headings of the satellite for selected latitudes. Changes in the satellite heading must be accounted for in the analysis of the data.

Table 1. Satellite Headings for Transit IV-A

Satellite latitude	30°	35°	40°	45°	50°	North
Satellite heading	23.8°	25.7°	28.2°	31.4°	35.7°	S-N passes
	156.2°	154.3°	151.8°	148.6°	144.3°	N-S passes

3. Receiver Locations Used

The receiver locations are shown in Figure 4 and summarized in Table 2.

Table 2. Receiver Locations

Location	Distance from Base Station	Azimuth from Base Station	Base Station
Chanute A.F.B.	34.6 km	28°	Monticello Road Field Station (Adcock) 40.016° N 88.325° W
Mansfield, Illinois	27.3	330°	"
A1	2.90	28°	"
A2	4.85	30°	"
A3	6.65	28°	"
Swine Farm	2.82	331°	Geophysical Observatory 40.069° N 88.225° W
Gartner House	2.92	32°	"
Wullenweber	15.1	261°	"
Ehler Farm	15.1	344°	"
Champaign Airport	9.25	263°	"

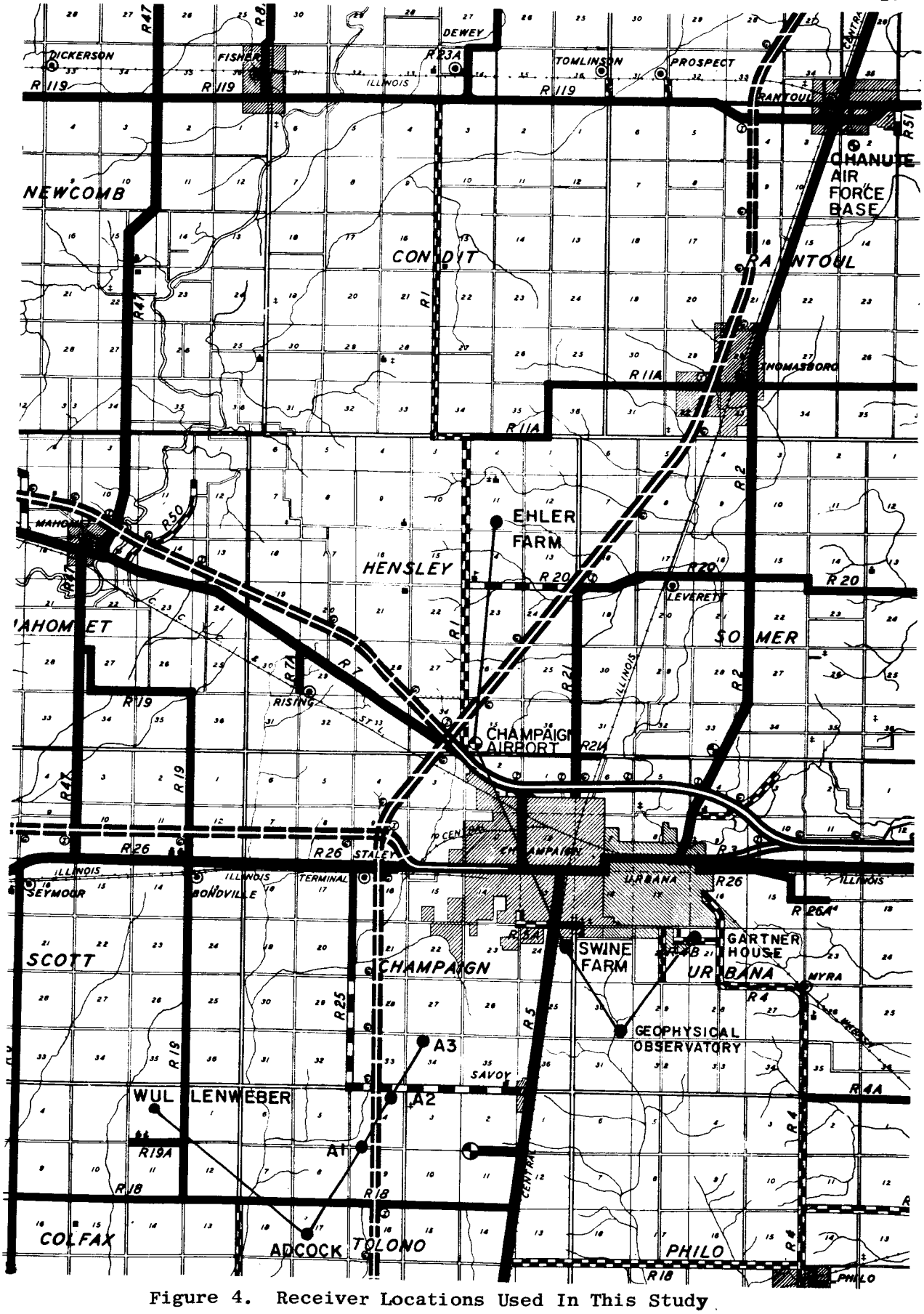

Figure 4. Receiver Locations Used In This Study

4. Characteristics of the Data Recording System

The AGC voltages of the receivers were recorded on an eight channel Sanborn strip chart recorder. This voltage was proportional to the logarithm of the signal strength. This simplifies data analysis because all the statistical properties of scintillation were given in terms of operations on the logarithmic amplitude.

Care was taken to insure that the data transmission system was linear. The time constant of the recording system was about 0.07 seconds which affected only the most rapid scintillation. The entire satellite recording system was designed to operate automatically, requiring only routine maintenance and daily programming.

Chapter III. Measurement of the Height and Size of the Irregularities

1. Irregularity Height Measurements Using the "Edge Effect"

The first measurements of irregularity height in this study were made by observing the easy-to-interpret "edge effect." Sharp transitions from scintillation to Faraday rotation or vice-versa were often seen to occur in a second or less. With receivers spaced 25 or 35 kilometers along the sub-satellite path it was possible to measure the ground velocity of the "edge" of the scintillation pattern. Figure 3 illustrates the geometry of these measurements. The heights observed at the University of Illinois were between 320 and 430 km. At College, Alaska, heights from 145 to 1000 km were observed on 23 satellite passes by the same method [Basler and DeWitt, 1962]. Table 2 shows the results of the observations at Urbana.

Table 2. Scintillation Heights Measured Using Sharp Transitions

Date	Time CST	Satellite	Receiver Spacing km.	T. Sec.	Scintillation Height km.
3 Feb. 1960	2000	EXPLORER VII	9.2	0.5 $\pm$ 0.1	412 $\pm$ 23
10 Nov. 1960	0543	TRANSIT II-A	34.6	5.25 $\pm$ .25	395 $\pm$ 10
31 Aug. 1961	2312	TRANSIT IV-A	34.6	7.0 $\pm$ 0.5	345 $\pm$ 15
8 Oct. 1961	2327	TRANSIT IV-A	27.3	7.25 $\pm$ .75	320 $\pm$ 20
12 Oct. 1961	2222	TRANSIT IV-A	27.3	4.5 $\pm$ .25	429 $\pm$ 13
13 Oct. 1961	2239	TRANSIT IV-A	27.3	4.5 $\pm$ .75	429 $\pm$ 39

Attempts were made to determine irregularity heights by the transition edge method for data recorded at Urbana, Illinois, and Huntsville, Alabama, using the satellites Explorer VII (1959 Iota) and Nora Alice I (1961 Alpha Kappa). However, the method can be used only if the satellite travels in the direction of a line joining the observing points, and Explorer VII passed at a 45^{o} angle to the line joining the towns, nullifying the experiment. While the path of Nora Alice I was satisfactory, its maximum height was only 350 km, the average height of the F-region irregularities themselves, and no useful information was obtained.

Table 2 shows a spread of 110 km in heights observed, but since measurements could be obtained only at the times of sharp transition, the method was inadequate for thorough analysis. Therefore observations by the edge effect method were discontinued and the cross correlation method was investigated. It was found that this method permitted continuous measurements of irregularity height during an entire satellite passage.

2. Irregularity Height Measurements Using Cross-Correlation

The geometry of cross-correlation measurement of irregularity height is the same as the geometry of edge effect measurements illustrated in Figure 3. However, the ground velocity of the radio signal strength pattern as a whole is measured, rather than the ground velocity of its edge, permitting continuous observation of the irregularity height, rather than discrete observations at the time of sharp transitions. A receiver spacing of approximately 3 km in the direction of scintillation pattern motion yields a very high cross-correlation between the signals at the two receivers, usually above 0.8. (Note that this spacing is much smaller than those

listed in Table 2.) When the cross-correlation is high, this function has approximately the width and shape of the autocorrelation function, shown by Kent [1959] and Swenson and Yeh [1961], but it is centered on some time shift T corresponding with the ground velocity of the drifting scintillation pattern. Theoretical calculations given in Chapter IV show that the value of irregularity height obtained by this method is approximately the height of the center of the region of irregularities.

One hundred thirty spaced-receiver recordings of Transit IV-A passages which displayed scintillation were examined in an attempt to determine the height behavior of scintillation-producing irregularities. These recordings were made between March, 1962 and December, 1963 on spaced receiver networks having two, three, and four receivers. Graphical cross-correlation was used to determine the time shift T for all scintillation occurring above an elevation of 30^{o}. From this time shift the pattern ground speed and irregularity height are found.

The observed time shifts on the Swine Farm--Geophysical Observatory baseline, for example, varied from 0.1 to 3.4 seconds, corresponding with ground pattern speeds from 28 to 0.83 km/sec or irregularity heights from 800 to 90 km. For elevation angles above 35^{o} the plane-earth formula

$$h_i = H_s v_g/(v_g + v_s) \qquad (1)$$

where h_i = irregularity height, v_g = pattern velocity on the ground, H_s = satellite height, v_s = satellite velocity

is valid without correction for satellites less than 1000 km high, such as Transit IV-A.

Due to the anistropy of the scintillation pattern, a difference of a few degrees between the satellite heading and the baseline of the receivers can cause large errors, if the direction of the pattern elongation is near the direction of the baseline. (During the first and last part of each Transit IV-A pass the difference was 4 to 8 degrees. (see Table I.)) Figure 5, below, shows the two extreme situations. A small difference between the direction of the baseline and the direction of V_g results in no appreciable error for the case of 5a, but in 5b a correction must be applied. If a third receiver is placed somewhere off the baseline of the first two, the correction can be measured directly. However, if only two receivers are used, the correction must be calculated. Note that the effective baseline is determined by the conjugate diameter with respect to v_g of the characteristic ellipse. This point is fully discussed by Liszka [1963].

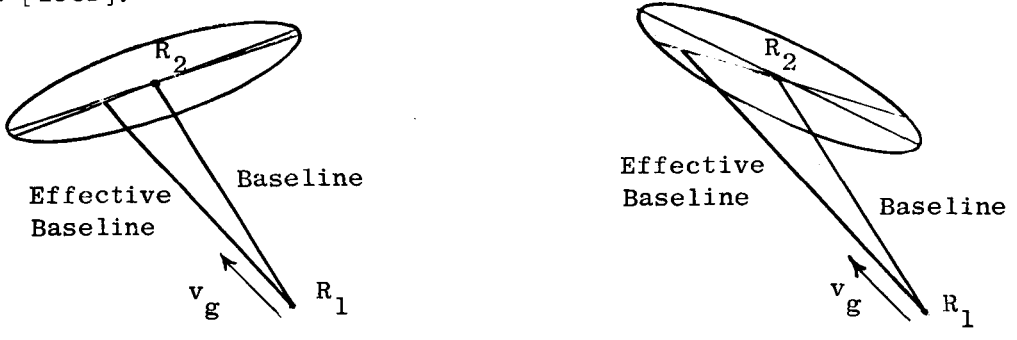

a b

Figure 5. Spaced Receiver Geometry for Irregularity Height Measurement

The accuracy of these height measurements is limited by the accuracy of measurement of the scintillation pattern ground speed. Errors in the measurement of v_g due to geometrical effects have been compensated for when necessary in the data analysis. The only remaining source of error was in measuring the cross correlation time shift T. T was generally measured to within $\pm$ 0.05 seconds, which is equivalent to $\pm$ 15 km at a height of 350 km.

In many of the observations the ground pattern velocity was more or less variable during the pass. These variations were followed by reducing the cross-correlation sample length to 10 seconds. They are interpreted as changes in irregularity height as a function of position. In a few cases, the scintillation was abnormally violent and the records could not be analyzed, because there was little or no correlation between the signals at the two receivers. The scintillation-producing region is believed to be much thicker or much more strongly irregular than normal at such times. Chapter IV examines this phenomenon in greater detail.

Figure 6 shows 13 examples which illustrate the main features of the irregularity height behavior found in the 130 height measurements. These measurements indicate that the irregularity height in the F-region was variable about one-third of the time and fairly uniform about two-thirds of the time. This is in general agreement with the findings of Jespersen and Kamas [1963]. Height variations may be gradual or abrupt. Combinations of height gradient regions and level regions were observed. Small patches of irregularities were seen, sometimes at a constant height, as on March 8, 1963 (see Figure 6), and sometimes at different heights.

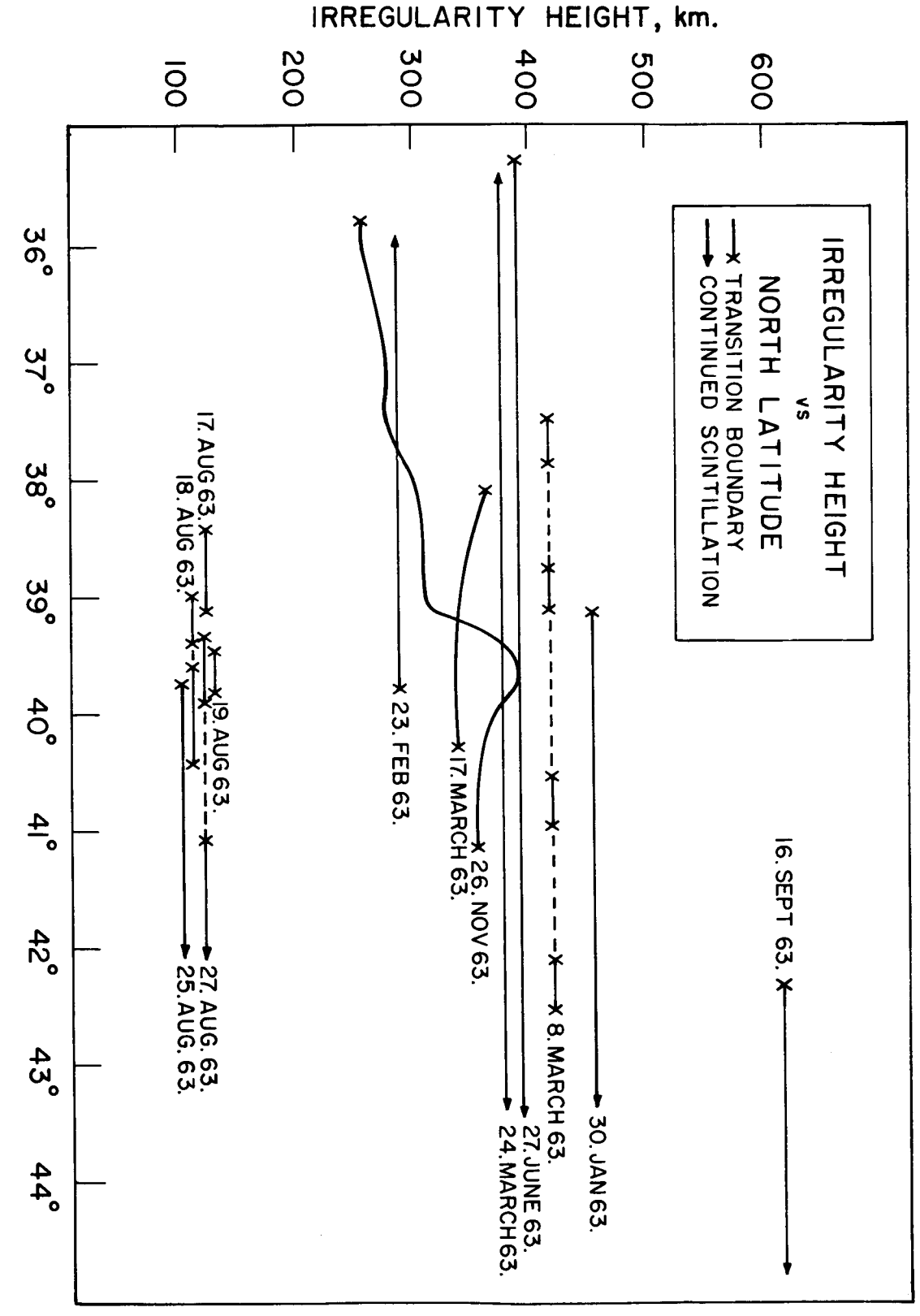

Figure 6. Thirteen Typical Examples of the 130 Height Measurements

Below 130 km, height variations were not observed. E-region irregularities were often very patchy, as shown by Figure 6.

Simultaneous irregularity height measurements made with spaced receivers on both 54 and 150 mc gave the same heights, within the accuracy of the measurements. A similar observation was made by Jespersen and Kamas [1963]. As predicted by the model used in Chapter IV based on the assumption of single scatter theory, we find height measurement is independent of frequency

Irregularity height distributions were prepared for each three-hour interval of the day. These distributions plus a composite distribution which includes all the data in one histogram, are shown in Figure 7. The diurnal changes in the irregularity height distributions are immediately apparent from Figure 7. Conclusions from this figure are as follows. At night, most of the scintillation is caused by F-region irregularities. At midday, most scintillation is caused by E-region irregularities. The diurnal variation of the incidence of F-region scintillation is very similar to the diurnal variation of the incidence of spread-F as shown by Shimazaki [1959]. The diurnal variation of E-region scintillation is very similar to the diurnal variation of sporadic-E as shown by Thomas and Smith [1959].

A strong positive correlation was found between the incidence of both E and F-region satellite scintillation and E and F-region irregularities observed on ionograms, when the scintillation was within 45^{o} of the zenith at the ionosonde and below the F-region maximum. The correlation was made by checking the ionograms corresponding with approximately 160 satellite passages recorded between April and November, 1963. The ionograms were

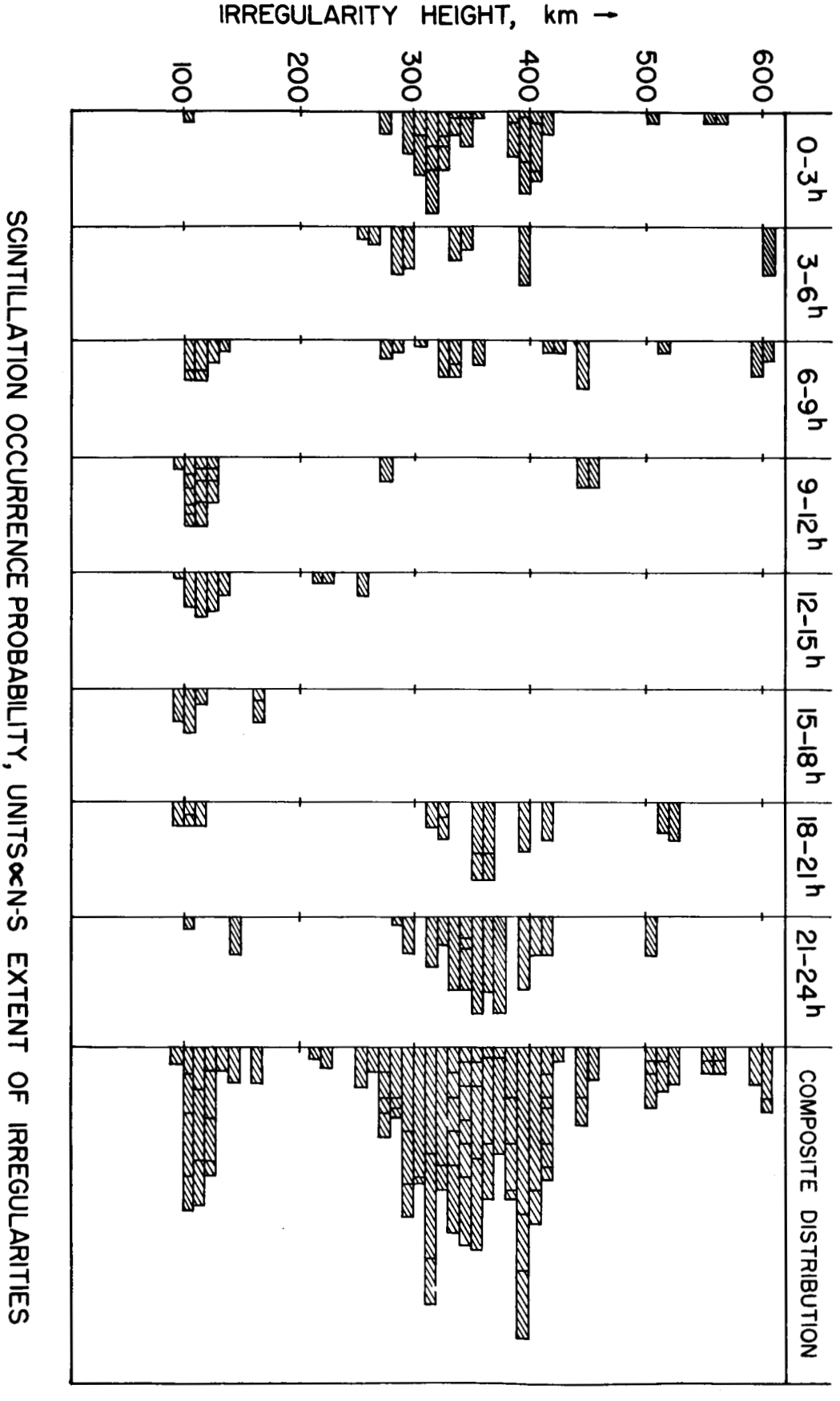

Figure 7. The Height Distribution of Irregularities Responsible for Satellite Scintillation

taken at Urbana, Illinois and at Anderson, Indiana, 200 km east of Urbana. On days when scintillation was observed in the F-region, spread-F was observed on the corresponding ionogram over 90 percent of the time. Similarly, when E-region scintillation was observed, sporadic-E was observed over 90 percent of the time. On one day, when the satellite showed patches of both E-region and F-region scintillation, both sporadic-E and spread-F appeared on the ionogram. On the other hand, there were many cases where spread-F or sporadic-E was observed on the ionogram and the corresponding satellite passage showed no scintillation. It is believed that this last phenomenon is caused by the "patchiness" of the irregularity regions. (When the ray to the satellite does not pass directly through the region of irregularities, no scintillation is observed.) This analysis confirms the earlier belief that scintillation was correlated with spread-F [Yeh and Swenson, 1959]. It is probable that correlation with sporadic-E was previously in doubt [deMendonca et al., 1960] because E and F-region scintillation had not yet been differentiated.

Figure 7 shows that, averaged over a long period of time, irregularity heights are broadly distributed in the F-region, but with most of the irregularities between heights of 300 and 400 km. E-region irregularities are much more narrowly distributed. Most of them fall between heights of 100 and 125 km. There are very few irregularities between 125 and 290 km, although occasional examples may be found in the figure. Balsley [1964] has observed thin irregularity layers in this height range using the incoherent scatter radar at Jicamarca, Peru.

Over a shorter interval of time the F-region irregularities may be concentrated in a narrower height range than that shown in Figure 7. For

example, a distribution of irregularity heights was prepared from approximately the first 25 percent of the data shown in Figure 7. This initial analysis showed that irregularities were distributed over about the same height range shown in Figure 7, but there was a much greater concentration of irregularities near the center of the range, i.e. the distribution had a distinct maximum near 350 km in contrast to the rather broad maximum of Figure 7. This distribution curve was presented earlier by Yeh, Swenson and McClure [1963], and later published in a modified form by Yeh and Swenson [1964]. The modification was made because the original distribution was based on the number of minutes of scintillation observed at each height, which tends to over-emphasize irregularities at lower heights. That is, an irregularity patch of a given size is observed for a longer time if it is low since the ray to the satellite has a lower velocity at lower heights. The distribution in Figure 7 is based on the spatial extent of the irregularities and gives a true indication of the relative incidence of irregularities at different heights.

The diurnal variation shown in Figure 7 indicates that the irregularity heights in the F-region tend to be distributed more broadly in the hours after midnight than in the hours before midnight. Attempts to find seasonal differences in the irregularity height behavior failed. Variations within any season were very large and there were not sufficient data to show conclusively that one season was any different from another. The irregularity heights sometimes had a tendency to remain nearly constant for a few days, but at other times varied widely from day to day. No other systematic variations in the seasonal or day-to-day irregularity height behavior were found.

Jespersen and Kamas [1963] reported a gradual increase of the average irregularity height to the north for 10 nighttime satellite passages which showed no discontinuities in height and for which three or more values of height were available for each pass. Their method of analysis was the same as that used here, except that they computed the cross-correlation function at discrete times (20-60 seconds apart). Figure 6 of their report shows a linear height increase of 13 km per 100 km to the north. This line was fitted by least squares to 43 height measurements from the ten passes. This figure could be interpreted as implying that, in individual cases where irregularity heights are non-discontinuous, there is a gradual increase in height to the north. In the present study, irregularity heights were measured continuously during all periods of scintillation. The results indicate that during an individual pass the most probable height gradient is near zero. Figure 6 of this report indicates that height gradients to the north and the south do exist, but are seldom uniform for more than 50-100 km. The average height of all F-region scintillation does seem to increase slightly to the north. However, this does not appear to be due to uniform layers of irregularities gently sloping upwards to the north, but to irregularity patches, large and small, being higher, on the average, in the north. Table 3 lists the observed average height of all F-region irregularities as a function of latitude.

Table 3. Average Irregularity Heights

North Latitude	Number of Observations	Average Irregularity Height
36^{o}	26	336 km
37^{o}	30	335 km
38^{o}	35	338 km
39^{o}	44	355 km
40^{o}	48	351 km
41^{o}	42	354 km
42^{o}	46	357 km
43^{o}	36	381 km
44^{o}	41	390 km

3. Irregularity Orientation and Size Measurements

To measure the orientation and size of a scintillation pattern on the ground, data from at least three non-colinear receivers is needed. The geometry of these measurements is thoroughly discussed by Liszka [1963b]. Briefly, the relative time shifts of the receiver outputs are used to determine the magnitude of the pattern drift velocity and the direction of orientation of the "line of maximum" [Liszka, 1963b]. The direction of the drift is antiparallel with the satellite velocity vector. For an elliptical pattern, the line of maximum is not the major axis but the conjugate diameter with respect to v_g of the characteristic ellipse. When the pattern is elongated by only 2 or 3:1 this difference is important, but for elongations greater than 5:1 it is negligible. The

cross-correlation of the receiver outputs can be used to determine the size of the pattern on the ground. This is discussed below with the aid of Figure 8.

Again in this study, as in previous studies, the measured orientation of the ground pattern elongation was always approximately the same as the orientation of the ground projection of the earth's magnetic field. This projection is the line of intersection of the ground plane and the plane determined by a ray to the satellite and a magnetic field line at the irregularity height. The measured orientation was observed to change consistently during a pass in a manner that could be called the "sundial effect." It is believed that this term was originally used by Professor S. A. Bowhill [private communication]. It does not seem to have appeared in the literature before.

For low elevation angles the ground pattern can become highly elongated. The straightness of the line of maximum may be checked by using a network of four or more receivers (Figure 8). When this was done for highly elongated patterns, there was high correlation between all receiver outputs. On every observation, the time shifts indicated that the line of maximum was straight. Further, the individual fades on the records were displaced by exactly the same amount, indicating that the individual irregularities were parallel with each other.

Table 4 shows the pattern size in the direction of its motion deduced from v_g and the fading rate. The example of October 19 shows the change in apparent size which could be expected from the change in the angle between v_g and the pattern orientation, assuming the pattern had a constant size during this time.

Table 4. Irregularity Size in the Direction of Pattern Motion

Date 1963	Time CST	Irregularity Height, km	Satellite Azimuth	Satellite Elevation	Angle, v_g to Major Axis	Pattern Size, km
Oct. 5	0203	300	89°	79°	58°	2.5
Oct. 7	0232	330	235°	37°	60°	2.4
Oct. 13	0026	325	157°	53°	15°	1.9
Oct. 19	2233	330	83°	69°	74°	2.0
	2234	330	120°	55°	59°	2.3
	2235	330	132°	39°	34°	3.3
Aug. 26	1016	105	36°	87°	75°	1.7
Aug. 27	1029	110	50°	92°	81°	1.5

To determine the size of the pattern in any direction other than the direction of satellite motion it is necessary to use cross-correlation. Since the scintillation pattern changes as it drifts, the receivers must be spaced in approximately the direction of the pattern orientation, so that the effect of this change on the cross-correlation is not too great. Also, in the interests of accuracy, the spacing distance must be such that the cross-correlation is neither too high nor too low. Therefore any network of three or four receivers can be used to find the pattern size for only a limited range of pattern orientations and sizes. Figure 8 illustrates favorable and unfavorable geometries for measuring irregularity size.

Figure 8a shows an ideal situation for measuring the size of the irregularity on the ground, since the correlation between the signals at R_1 and R_4 would be ~0.5 and the time delay would be ~0. However, if R_4

were missing, the measurement would be less accurate, since the cross-correlation between R_1 and R_3 would be greater than 0.5. The situation shown in Figure 8b is unfavorable for accurate irregularity size measurements. While here the cross-correlation between R_1 and R_3 might be as low as 0.5, the time delay would be large. Therefore, it would be impossible to separate the effect of pattern size and the effect of pattern change, because both govern the cross-correlation observed under these conditions.

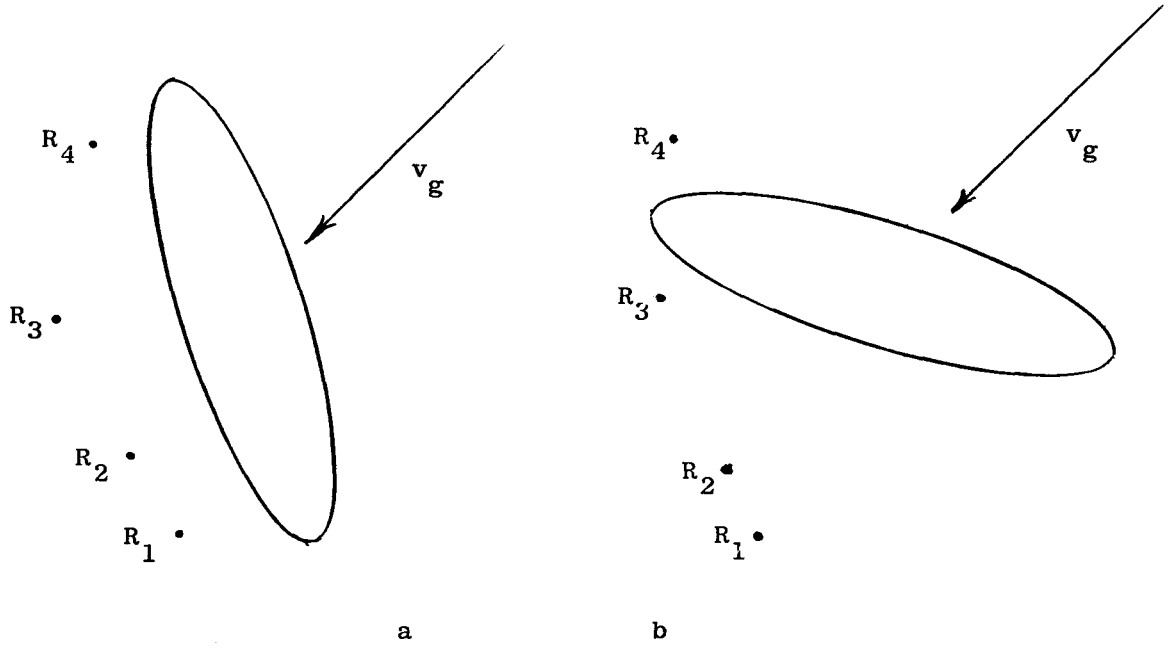

Figure 8. Geometry of the Cross-Correlation Method of Measuring Irregularity Size

A few examples of E and F-region scintillation were chosen and examined to find the approximate dimensions of the ground pattern. The direction of elongation of both the E and F-region patterns was consistent with the "sundial" hypothesis and their size indicated that they were caused by

approximately 1 × 10 km field-aligned irregularities. No further investigation of this subject was attempted. The relation between the pattern size and the size of the irregularity in the ionosphere is discussed by Yeh [1962].

Chapter IV. Thickness of the Region of Irregularities

1. Derivation of the Cross-Correlation Function for Satellite Scintillation

The height of the inhomogeneous region of the ionosphere responsible for satellite scintillation has been found by measuring the ground velocity of the scintillation pattern. When measuring the ground velocity with spaced receivers it is observed that the satellite signal strength pattern changes as it drifts, and that the rate of change is variable. For example, over a distance of 10 km in the direction of the satellite velocity, the cross-correlation between the signals observed is usually in the range of 0.3 to 0.7, although it is sometimes above or below this range. It will be shown here that this phenomenon can be related to the thickness of the irregularity region.

A model ionosphere having a uniform slab of irregularities is chosen. The irregularities are chosen to be Gaussian with ellipsoidal symmetry. Starting with the general correlation function of Yeh [1962], a solution for the geometry of the spaced receiver experiment is obtained. The result is a concise function expressing the normalized cross-correlation for satellite signals observed at spaced receivers.

James [1962] has derived, from the diffraction theory, a relationship between the thickness of the irregularity region and V_c, the fading velocity of Briggs et al. [1950]. It will be shown that James' formula can also be derived from the scattering theory presented here. James' formula was derived for a region of irregularities with a Gaussian vertical distribution, but a uniform slab of equivalent thickness will be shown to give the same result.

Yeh [1962] has computed expressions for some of the statistical properties of a spherical wave propagated through a random medium. He has assumed that the irregularities in the random medium are so weak that only first order scattering is important (Born approximation), and also that the medium is slowly varying. The scalar Helmholtz wave equation is expanded in a series (perturbation method). A solution for the first order term is obtained. From this, general correlation functions for phase departure and logarithmic amplitude are found. He has evaluated the general correlation functions

$$\langle Q(\bar{x}_1)\, Q(\bar{x}_2)\rangle = (r_1 r_2\, \epsilon^2 \langle \mu^2 \rangle / 4\pi^2) \int_{V_1} \int_{V_2} \frac{\sin(r_1' + R_1 - r_1)}{r_1' R_1} \cdot \frac{\sin(r_2' + R_2 - r_2)}{r_2' R_2}\, \rho_\mu(\bar{x}')\, d^3 \bar{x}_1'\, d^3 \bar{x}_2' \qquad (2)$$

$$\langle S(\bar{x}_1)\, S(\bar{x}_2)\rangle = (r_1 r_2\, \epsilon^2 \langle \mu^2 \rangle / 4\pi^2) \int_{V_1} \int_{V_2} \frac{\cos(r_1' + R_1 - r_1)}{r_1' R_1} \cdot \frac{\cos(r_2' + R_2 - r_2)}{r_2' R_2}\, \rho_\mu(\bar{x}')\, d^3 \bar{x}_1'\, d^3 \bar{x}_2' \qquad (3)$$

to find values of the phase and amplitude scintillation index and the autocorrelations of phase and amplitude, assuming a Gaussian autocorrelation function $\rho_\mu(\bar{x}')$ for the ionospheric irregularities. We shall make the same assumption and evaluate the general expressions for the cross-correlation as found in spaced receiver measurements.

The geometries used by Yeh and the geometry used in the present study are shown in Figure 9. The notation of Equations (2) and (3) is explained in Figure 9a. The subscripts on the terms r, r' and R specify the elementary volume $d^3\bar{x}$ to which they correspond. The correlation of the ionospheric irregularities ρ_μ is a function of the distance $\bar{x}'$ between volumes $d^3\bar{x}_1$ and $d^3\bar{x}_2$. All lengths in (2) and (3) are normalized by the wave number $k = \omega < n > /c$.

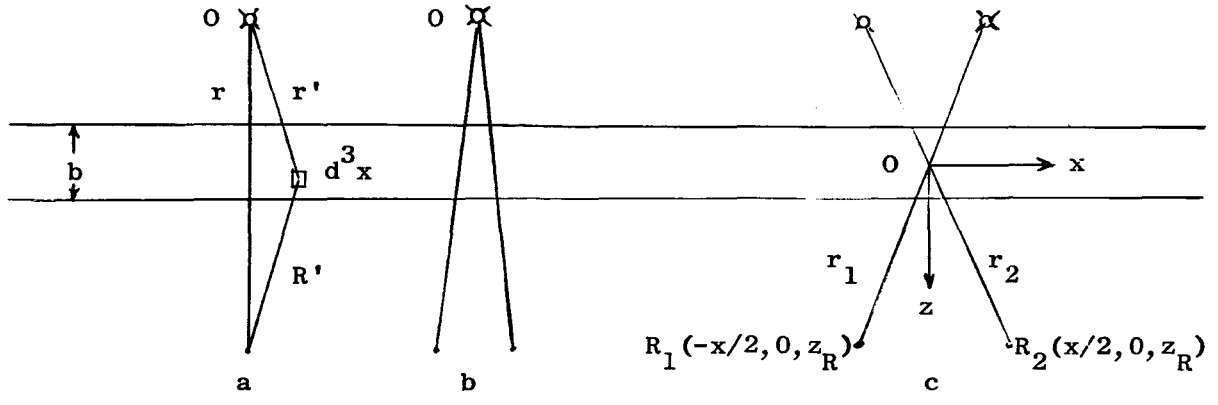

Figure 9. Geometries Used For Computing the Statistical Properties of Scintillation

The derivation of the cross-correlation function is similar to the derivation of the autocorrelation function (Section 6 of Yeh [1962]). The same approximation for the phase difference between the direct and scattered wave can be used.

$$(r_1' + R_1 - r_1) \simeq [y_1'^2 + (x_1' - xz_1'/2z_R)^2]/2\zeta_1' \qquad (4)$$

$$(r_2' + R_2 - r_1) \simeq [y_2'^2 + (x_2' - xz_1'/2z_R)^2]/2\zeta_2' \qquad (5)$$

where

$$\zeta_1 = (z_1' - z_T)(z_R - z_1')/(z_R - z_T) \qquad (6)$$

$$\zeta_2 = (z_2' - z_T)(z_R - z_2')/(z_R - z_T) \qquad (7)$$

The origin of the coordinate system has been moved from the satellite to the center of the slab. When they appear in the denominator of (2) and (3), let $r' \tilde{=} z' - z_T$ $\quad R \tilde{=} z_r - z'$. Define

$$I_3 = (\pi/\epsilon^2 < \mu^2 >)(< Q_1 Q_2 >_{CC} + < S_1 S_2 >_{CC}) \tag{8}$$

$$I_4 = (\pi \epsilon^2 < \mu^2 >)(< Q_1 Q_2 >_{CC} - < S_1 S_2 >_{CC}) \tag{9}$$

Putting the general expressions (2) and (3) into the above definitions we obtain

$$I_3 = \frac{1}{\pi} \int\int \frac{\rho_\mu(\bar{x}')}{4\zeta_1' \zeta_2'} \cos \left(\frac{y_1'^2 + (x_1' - xz_1'/2z_R)^2}{2\zeta_1'} \right.$$

$$\left. - \frac{y_2'^2 + (x_2' + xz_2'/2z_R)^2}{2\zeta_2'} \right) d^3\bar{x}_1 \, d^3\bar{x}_2 \tag{10}$$

$$I_4 = -\frac{1}{\pi} \int\int [\rho_\mu(\bar{x}')/4\zeta_1'\zeta_2'] \cos \left(\frac{y_1'^2 + (x_1' - xz_1'/2z_R)^2}{2\zeta_1} \right.$$

$$\left. + \frac{y_2'^2 + (x_2' + xz_2'/2z_R)^2}{2\zeta_2'} \right) d^3\bar{x}_1' \, d^3\bar{x}_2' \tag{11}$$

In order to integrate these expressions, we transform coordinates to the relative and center of mass systems

$$x' = x_2' - x_1', \quad y' = y^2 - y_1', \quad z' = z_2' - z_1' \tag{12}$$

$$\alpha' = (x_1' + x_2')/2, \quad \beta' = (y_1' + y_2')/2, \quad \gamma' = (z_1' + z_2')/2 \tag{13}$$

Integrating with respect to α' and β', we have, by Dwight 859.5

$$I_3 = \int_{\gamma'=-b/2}^{b/2} \int_{z'=-b}^{\infty} \int_{y'=-\infty}^{\infty} \int_{x'=-\infty}^{\infty} \frac{\rho_\mu(\bar{x}')}{2(\zeta_1' - \zeta_2')} \sin \frac{y'^2 + (x' + x\gamma'/z_R)^2}{2(\zeta_1' - \zeta_2')} \, dx'dy'dz'd\gamma' \tag{14}$$

$$I_4 = \int_{\gamma'=-b/2}^{b/2} \int_{z'=-b}^{b} \int_{y'=-\infty}^{\infty} \int_{x'=-\infty}^{\infty} \frac{\rho_\mu(\bar{x}')}{2(\zeta_1' + \zeta_2')} \sin \frac{y'^2 + (x' + x\gamma'/z_R)^2}{2(\zeta_1' + \zeta_2')} \, dx'dy'dz'd\gamma' \tag{15}$$

Except for the limits, these integrals are the same as (56) and (57) of Yeh [1962]. Assume the autocorrelation of the random part of the dielectric constant in the ionosphere to be Gaussian with ellipsoidal symmetry.

$$\rho_\mu(\bar{x}) = \exp - (x^2/\ell_x^2 + y^2/\ell_y^2 + z^2/\ell_z^2) \tag{16}$$

The slab of irregularities is much thicker than ℓ_z. Thus the limits of integration with respect to z' can be extended from $-\infty$ to ∞ in (14) and (15). Substituting the correlation (16) and expressing the sine in complex notation

$$I_3 = \mathrm{Im} \int_{-b/2}^{b/2} \int_{-\infty}^{\infty} \int_{-\infty}^{\infty} \int_{-\infty}^{\infty} \frac{\exp(-z'^2/\ell_z^2)}{2(\zeta_1' - \zeta_2')} \exp\left[-y'^2/\ell_y^2 + jy'^2/2(\zeta_1' - \zeta_2')\right]$$

$$\exp\left[-x'^2/\ell_x^2 + j(x' + x\gamma'/z_R)^2/2(\zeta_1' - \zeta_2')\right] dx'dy'dz'd\gamma' \tag{17}$$

$$I_4 = \mathrm{Im} \int_{-b/2}^{b/2} \int_{-\infty}^{\infty} \int_{-\infty}^{\infty} \int_{-\infty}^{\infty} \frac{\exp(-z'^2/\ell_z^2)}{2(\zeta_1 + \zeta_2)} \exp\left[-y'^2/\ell_y^2 - jy'^2/2(\zeta_1' - \zeta_2')\right]$$

$$\exp\left[-x'^2/\ell_x^2 + j(x' + x\gamma'/z_R)^2/2(\zeta_1' + \zeta_2')\right] dx'dy'dz'd\gamma' \qquad (18)$$

The x' integration is of the form Dwight 863.3 and the y' integration is of the form Dwight 861.3. Integrating with respect to x' and y',

$$I_3 = \mathrm{Im} \int_{-b/2}^{b/2} \int_{-\infty}^{\infty} \frac{\pi \exp(-z'^2/\ell_z^2) \exp(-x^2\gamma'^2/\ell_x^2 z_R^2)\, dz'd\gamma'}{\left[2z'(2\gamma' - z_R - z_T)/\ell_x^2(z_R - z_T) - j\right]^{1/2}\left[2z'(2\gamma' - z_R - z_T)/\ell_y^2(z_R - z_T) - j\right]^{1/2}} \qquad (19)$$

$$I_4 = \mathrm{Im} \int_{-b/2}^{b/2} \int_{-\infty}^{\infty} \frac{\pi \exp(-z'^2/\ell_z^2) \exp\left[-x^2\gamma'^2/(1 + jD_x)\ell_x^2 z_R^2\right] dz'\, d\gamma'}{\left[D_x - z'^2/\ell_x^2(z_R - z_T) - j\right]^{1/2}\left[D_y - z'^2/\ell_y^2(z_R - z_T) - j\right]^{1/2}} \qquad (20)$$

where the new terms D_x and D_y are the wave parameters, defined as

$$D_x = 4z_T z_R + 4\gamma'(z_R + z_T - \gamma')/\ell_x^2(z_R - z_T) \qquad (21)$$

$$D_y = 4z_T z_R + 4\gamma'(z_R + z_T - \gamma')/\ell_y^2(z_R - z_T) \qquad (22)$$

Since the size of the irregularities is much greater than one wavelength ($\ell \gg 1$), terms like $2z'(2\gamma' - z_R - z_T)/\ell^2(z_R - z_T)$ and $z'^2/\ell^2(z_R - z_T)$ are much less than unity and can be neglected. The z' integration is now of the familiar form Dwight 861.3. Integrating with respect to z'

$$I_3 = \pi^{3/2} \ell_z \int_{-b/2}^{b/2} \exp(-x^2\gamma'^2/\ell_x^2 z_R^2)\, d\gamma' \tag{23}$$

$$= \frac{\pi^2 \ell_z \ell_x z_R}{x} \operatorname{erf}\left(\frac{xb}{2\ell_x z_R}\right) \tag{23a}$$

$$I_4 = \pi^{3/2} \ell_z \operatorname{Im} \int_{-b/2}^{b/2} \frac{\exp(-x^2\gamma'^2/(1-jD_x)\,\ell_x^2 z_R^2)\, d\gamma'}{(D_x - j)^{1/2}\,(D_y - j)^{1/2}} \tag{24}$$

The wave parameters D are introduced and discussed by Yeh. The value of D in dimensionless units is approximately equal to the reciprocal of twice the phase difference between the direct wave and a wave scattered from a point $\ell_x/2$ or $\ell_y/2$ away from the direct ray at the height of interest. When the D's are very small the phase differences are very large, and we have Fresnel diffraction. For large D's, the phase differences are very small, and we have Fraunhofer diffraction.

For $D \gg 1$, $I_4 \tilde{=} 0$. Define the normalized cross-correlation functions for phase and logarithmic amplitude as

$$\rho_Q(x) = \langle Q_1 Q_2 \rangle_{CC} / \langle Q^2 \rangle \tag{25}$$

$$\rho_S(x) = \langle S_1 S_2 \rangle_{CC} / \langle S^2 \rangle \tag{26}$$

For the condition $D \gg 1$, Yeh has computed the mean square values

$$\langle Q^2 \rangle = \langle S^2 \rangle = \epsilon^2 \langle \mu^2 \rangle \pi^{3/2} \ell_z b/2 \tag{27}$$

Referring to equations (23) and (24), we have

$$\rho_Q(x) = \rho_S(x) = \pi^{1/2} \frac{\ell_x z_R}{bx} \operatorname{erf} \frac{xb}{2\ell_x z_R} \tag{28}$$

which approximates to

$$\rho_Q(x) = \rho_S(x) \simeq 1 - \frac{b^2 x^2}{12 \ell_x^2 z_R^2} \quad \text{for } bx \leq \ell_x z_R \tag{29}$$

$$\rho_Q(x) = \rho_S(x) \simeq \pi^{1/2} \frac{\ell_x z_R}{bx} \quad \text{for } bx \geq 3\ell_x z_R \tag{30}$$

Figure 10 shows that the latter approximation is valid whenever the cross-correlation is 0.5 or less.

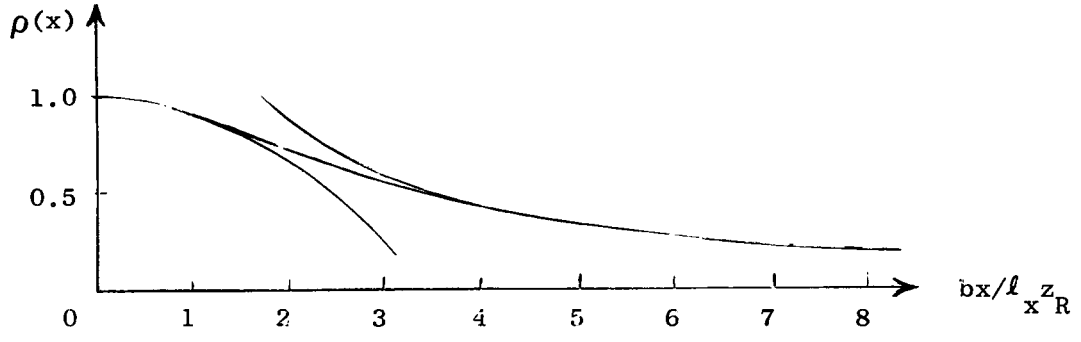

Figure 10. The Cross-Correlation Function for Fraunhofer Diffraction

The actual values of D which obtain at 54 mc for scintillation from Transit IV-A are between 0.3 (E-region scintillation) and 0.8 (F-region scintillation). For these values of D, I_4 is a complex error function. Assuming $D_x = D_y = D$ = constant over the height range of interest,

$$I_4 = \pi^{3/2} \ell_z \, \mathrm{Im} \frac{1}{D-j} \int_{-b/2}^{b/2} \exp -x^2\gamma'^2/(1+jD)\ell_x^2 \, z^2 d\gamma' \qquad (31)$$

$$I_4 = \pi^{3/2} \ell_z \, u \, \mathrm{Re} \int_{-b/2}^{b/2} \exp -(u - jv) \, x^2\gamma'^2/\ell_x^2 \, z^2 \, d\gamma' \qquad (32)$$

where

$$u = \frac{1}{1 + D^2} , \qquad v = \frac{D}{1 + D^2} \qquad (33)$$

For values of $D \ll 1$, the mean square values are computed by Yeh.

$$\langle Q^2 \rangle = \epsilon^2 \langle \mu^2 \rangle \pi^{1/2} \ell_z \, b$$

$$\langle S^2 \rangle = \epsilon^2 \langle \mu^2 \rangle \pi^{1/2} \ell_z \, D^2 \, b/2$$

Thus the cross-correlation functions are the same as for the condition $D \gg 1$. For finite values of D, the periodic part of I_4 will cause the cross-correlation functions to depart slightly from their values at $D \gg 1$. However, for the actual values of $D < 0.8$ at 54 mc, the departure will not be large and the functions, equation (28), (29), and (30) can be used.

We are now in a position to examine the meaning of the cross-correlation function in greater detail than was possible before. The function we have computed is the value of the cross-correlation when the rays to the satellite from the receiver positions R_1 and R_2 cross the center of the region of irregularities (see Figure 9). This is exactly the geometry assumed for

making irregularity height measurements by the cross-correlation method described in Chapter III (see Figure 3). This method of measuring irregularity heights is based on the time shift required for maximum cross-correlation of the signals observed at spaced receivers. If the direct rays to the satellite (Figure 9) cross at any height other than the center of the region of irregularities, the limits of the γ' integration in equations (14) through (24) will be unsymmetrical and the values of I_3 and I_4 determined by equations (23) and (24) will not be maximal, although the integration will still be over a total range b. However, if the rays cross at the center of the region of irregularities, I_3 and I_4, and therefore the cross-correlation functions, have a maximum because the limits are symmetrical. Hence the cross-correlation method yields the average height for a uniform slab of irregularities.

2. Comparison of the Cross-Correlation Function with an Intuitive Approximation

It has been found that an intuitive approximation to the problem gives almost the same cross-correlation functions as the rigorous calculation above. This approach is as follows: since most of the signal on the ground is due to scatterers in the first Fresnel zone, we may assume that the cross-correlation function is proportional to the common volume of the two cylinders shown below.

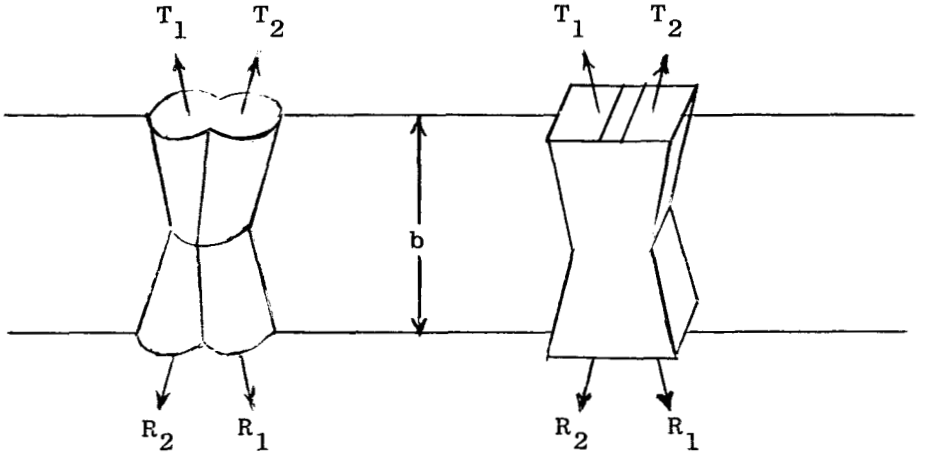

Figure 11. Cylindrical Intersection Approximation to the Cross-Correlation Function

We now compute the normalized value of the common volume of the two cylinders and compare with scattering theory.

Circular-Cylinder Approximation	Square-Cylinder Approximation	Scattering Theory
	$\rho(x) = 1 - \frac{bx}{8z_R R_f}$	$\rho(x) = 1 - \frac{b^2 x^2}{12 \ell_x^2 z_R^2}$
	$x \leq 4 \frac{z_R R_f}{b}$	$bx < \ell_x z_R$
$\rho(x) = \frac{16}{3\pi} \frac{z_R R_f}{bx}$	$\rho(x) = \frac{2 z_R R_f}{bx}$	$\rho(x) = \pi^{1/2} \frac{\ell_x z_R}{bx}$
$x \geq 4 \frac{z_R R_f}{b}$	$x \geq 4 \frac{z_R R_f}{b}$	$bx > 3 \ell_x z_R$

The square cylinder approximation leads to a correlation which starts with a linear decay and becomes hyperbolic where $\rho(x) = 1/2$. The scattering theory leads to a correlation which starts with a parabolic decay and

becomes hyperbolic somewhat before $\rho(x) = 1/2$. The circular-cylinder approximation also becomes hyperbolic in about the same region. The constants for each of the three cases are slightly different, but the resultant curves are very similar.

3. Derivation of James' Formula from the Cross-Correlation Function

A formula for the thickness of the region of inhomogeneity was derived from the diffraction theory by James [1962]. It is given as

$$\Delta = \frac{v_c v_s H_s}{(v_s + v_g)^2} \tag{34}$$

where the irregularities are vertically distributed as $\exp [-(z-h)^2/4\,\Delta^2]$. V_c is the "fading velocity," defined as the ratio of the pattern size in the direction of motion to the average lifetime of an irregularity [Briggs et al., 1940].

In his derivation, James has made the assumption that the magnification parameter ℓ_x/ℓ_g (Figure 11b) is given by,

$$\ell_x/\ell_g = (H_s - h_i)/H_s \tag{35}$$

This is not always valid. (See Yeh [1962] for a discussion of the problem.) However, if we assume it to be true, we may derive James' formula from equation (30). The average lifetime of an irregularity T_o is defined as the time required to reduce the cross-correlation of the irregularity pattern to 0.5. T_o, the correlation distance x_o, the ground velocity of the irregularity pattern v_g and the pattern size in the direction of motion ℓ_g, are related as follows.

$$v_c = \ell_g / T_o = \ell_g / x_o / v_g \tag{36}$$

The hyperbolic approximation to the cross-correlation function, equation (30), is valid in the case where $\rho(x_o) = 0.5$, and it then yields

$$x_o = 2\pi^{1/2} \ell_x h_i / b \tag{37}$$

Inverting equation (1) we have

$$v_g = v_s \frac{h_i}{H_s - h_i} \tag{38}$$

Combining (36), (37) and (38)

$$b = 2\pi^{1/2} \ell_x v_c (H_s - h_i) / \ell_g v_s \tag{39}$$

Combining (35) and (39)

$$b = 2\pi^{1/2} v_c (H_s - h_i)^2 / v_s H_s \tag{40}$$

Using equation (38), we have

$$b = \frac{2\pi^{1/2} v_c v_s H_s}{(v_s + v_g)^2} = 2\pi^{1/2} \Delta \tag{41}$$

Thus the ratio of b, as defined in this chapter, and Δ, as defined by James, is the constant $2\pi^{1/2}$, when we use James' simplifying assumption (equation (35)). Furthermore, the thickness b' of a uniform slab, equivalent to James' Gaussian-shaped slab, is also $2\pi^{1/2} \Delta$, since

$$b' = \int_{-\infty}^{\infty} \exp[-(z - h)^2 / 4 \Delta^2] \, dz = 2\pi^{1/2} \Delta \tag{42}$$

Figure 12 below illustrates the relationship between the two slabs. The total area under the irregularity distribution curves is equal. Thus

Figure 12. a) The Irregularity Distribution of James and the Equivalent Rectangular Irregularity Distribution
b) The Geometrical Magnification of Ionospheric Irregularities

James' formula is a special case of the cross-correlation function derived in this chapter.

4. Application of the Cross-Correlation Function to Measurement of the Irregularity Region Thickness

Spaced receiver measurements made in this study show that for F-region irregularities, a typical irregularity pattern on the ground must drift approximately 10 km before the cross-correlation is reduced to 0.5. Using the cross-correlation function, equation (28), this corresponds with an irregularity region thickness b of approximately 120 km. Table 5 shows seven specific examples of cross-correlation data and the layer thickness deduced from them.

Table 5. Data on the Rate of Change of the Diffraction Pattern

Date 1963	Time CST	Irregularity Height	Satellite Elevation	Scintillation Index	Cross-Correlation	Distance x	Thickness b
Oct.5	0203	300 km	79°	.12	.46	15 km	76
Oct.13	0026	325	53°	.15	.4	6.4	185
Oct.19	2234	330	55°	.22	.45	9	119
					.29	16.8	
Oct.20	2246	330	60°	.11	.63	15	50
Oct.23	2142	470	52°	.36	.55	9	130
Aug.26	1016	105	36°	~.1	>.5	13	< 17
Aug.27	1029	110	50°	~.05	>.5	13	< 23

The cross-correlation function (equation (28)) was derived for the symmetric case (Figure 9), where the satellite is near the zenith. In actual practice, an approximation to this geometry must be used. The data in Table 5 refer to satellites near the point of closest approach, near which the cross-correlation function (28) should still give valid results. The example for October 19, 1963, shows that the cross-correlation was approximately an inverse function of distance, as predicted.

It was mentioned in Chapter III that occasional examples of very violent scintillation show little or no correlation using a 3 km receiver spacing. These examples would correspond with irregularity region thicknesses of more than 300 km. They were not included in Table 5 because the data did not permit accurate calculations of the cross-correlation and because such violent scintillation was very rare. It is possible that

multiple scattering had occurred on such occasions, and that the assumption of "weak" irregularities is therefore not valid. See Yeh [1962] and Yeh and Swenson [1964].

The E-region layer thickness observed on August 26 and 27, 1963, was too thin (less than 15 km) to be accurately measured with the 13 km receiver spacing used. It is known that E-region irregularity layers can be less than 5 or 10 km thick [Thomas and Smith, 1959]. The results of this chapter show that for such layers, receivers spaced about 25 km apart should still yield high cross-correlation and valid height measurements. However, due to slow decrease of the cross-correlation, such measurements would not be suitable for determining the thickness of thin E-region irregularity layers.

Jespersen and Kamas [1963] have used James' formula to determine the thickness of F-region irregularity regions. They have stated that the thickness ($4\ \Delta$) for 13 examples varies from 90 to 470 km. Their measurements were made with a triangular array of antennas spaced 1600 feet apart. Observations made in this study indicate that the cross-correlation observed with such a narrow spacing should be quite high, and Figure 10 shows that the slope of the cross-correlation curve under such conditions makes it very difficult to measure accurate values for v_c. Nevertheless, their values for the thickness of F-region irregularity layers are in fairly good agreement with the values obtained here.

Cohen and Bowles [1961] reported that equatorial F-region irregularities were in layers about 50 km thick. Their measurements were based on ionospheric propagation via scattering from the F-region of 50 mc pulses.

Other observers have measured the thickness of the irregularity layers responsible for satellite scintillation directly from equation (1). If it is assumed that this equation holds for individual irregularities, then a height distribution of individual irregularities during a single pass can be obtained from the distribution of ground velocities, because individual variations in the ground signal strength pattern drift at different velocities. Using this method Yerukimov [1962] reported the irregularities were distributed over regions 150 to 200 km thick for F-region scintillation, and Liszka [1963b] reported thicknesses from about 20 to over 800 km for E and F-region scintillation in the auroral zone. Hook and Owren [1962] found auroral zone irregularities vertically distributed in cylinders about 30 to 70 km wide in the north-south direction and extending from a height of approximately 100 km to at least 275 km, the height of the satellite. The cylinders were aligned approximately with the earth's magnetic field. It is believed that these studies all determined the irregularity region height and thickness by using the time shifts of similar fades on the recordings, rather than using the cross-correlation of a segment containing many fades, as in this report. Receiver spacings were about an order of magnitude smaller than those used in this study. Even so, their data seem to indicate that the cross-correlation observed in the auroral zone was quite low at times. To obtain these results under the assumptions of this chapter would require that the irregularity region be unrealistically thick, perhaps thicker than the distance from the earth to the satellite. The published data do not permit thickness calculations by the cross-correlation method (equation (30)), but seem to indicate

that unrealistic thicknesses might be obtained. Such a result would show that the assumption of single scattering from a slowly varying random medium, or one of the other assumptions of this chapter, is not valid.

Chapter V. Conclusions and Suggestions for Further Study

Spaced receivers can be used to measure the ground velocity and change of ground signal strength pattern produced by ionospheric irregularities. These measurements provide an excellent method of determining the heights and thicknesses of regions of irregularity responsible for satellite scintillation. A particular advantage of this approach is that measurements may be made continuously during a satellite passage, yielding information on the geographic variation of these parameters.

Prior to this study, data on the statistical variation of heights of scintillation-producing irregularities has been meager. It is believed that the observations and analysis contained herein substantiate the following conclusions:

(1) Most nighttime scintillation in temperate latitudes is caused by F-region irregularities as shown by previous studies. In addition, it was found that they lie mainly between 300 and 400 km in height.

(2) Most daytime scintillation in temperate latitudes is caused by E-region irregularities near 100 km in height. The connection between daytime scintillation and E-region irregularities has not been clear heretofore. It is probable that the reason previous studies tended to show the opposite (Lawrence et al., 1961) is because E and F-region scintillation had not been differentiated.

(3) When ionospheric irregularities producing satellite scintillation exist sufficiently close to an ionosonde, ionogram irregularities will be observed. This holds for both E and F-region irregularities.

(4) Sporadic-E and spread-F on ionograms are not necessarily accompanied by satellite scintillation.

(5) Above 130 km, irregularity heights often vary considerably, not only from day to day, but also during a single satellite pass. It is believed that the reasons for these variations will not be known until the origins of irregularities are better understood.

(6) Diurnal variations of E and F-region scintillation-producing irregularities are similar to the diurnal variations of sporadic-E and spread-F. No conclusions have been reached with regard to seasonal variations.

Theoretical calculations have been based upon the assumptions of single scattering from a uniform slab of ionospheric irregularities, a Gaussian auto-correlation of the dielectric constant with ellipsoidal symmetry (axes lying in and perpendicular to the horizontal plane), and a satellite position close to the zenith at the time of measurement. Under these assumptions, the cross-correlation method of measuring irregularity heights yields the average height of the slab of irregularities. The analysis also shows that the cross-correlation between the signals observed at receivers spaced in the direction of satellite motion is a monotone decreasing function dependent only upon the thickness and height of the region of irregularities, the size of the irregularities, and the receiver spacing. Further, when the cross-correlation is less than 0.5, it varies inversely with the irregularity region thickness and receiver spacing. James' formula is a special case of the cross-correlation function derived here (equation (30)).

While equations (28), (29), and (30) assume Fraunhofer diffraction, they are approximately valid for F-region scintillation at the frequency used (54 mc). Further, equations (23) and (24) hold for any diffraction assumption and can be used to derive correlation functions for lower frequencies.

Measurements indicated that, for F-region scintillation, the cross-correlation of the scintillation pattern over a baseline of 10 km usually ranges from 0.3 to 0.8. This corresponds with irregularity region thicknesses between 50 and 250 km. Typical thicknesses were in the neighborhood of 120 km. These values are only slightly lower than those obtained by Jespersen and Kamas [1963] using James' formula.

The reason for the variation of the F-region irregularity heights is an important area for further research. Simultaneous measurements of irregularity height and other details of scintillation, such as irregularity strength, size, and layer thickness should be made along with other geophysical parameters. Perhaps it will be found that ionospheric irregularities are closely correlated with electron precipitation [Yeh and Swenson, 1964] or with sub-visual red-arcs in the ionosphere [Megill and Carlson, 1964].

An attempt was made to correlate some Explorer VII data showing strong, patchy scintillation on November 27 and 28, 1959, with Geiger tube counts of electron precipitation observed on the same passages. The counting rate was high and nearly constant throughout the November 27 passage. During the November 28 passage, it showed a steady increase as the satellite was passing the latitude of the University of Illinois on a northbound heading. The counting data were furnished by Professor J. A. Van Allen (private

communication). The counting rates showed no detailed variations corresponding with the variations of scintillation index. However, the Anton 302 Geiger tube used responds only to electrons with energies greater than 30 kev [Ludwig and Whelpley, 1960], and it is possible that a different type of counter might show a relationship between scintillation and electron precipitation in some other energy range.

A striking increase in scintillation has been observed on signals propagated through sub-visual red arcs [Roach, 1963]. His observations could be advanced by using the techniques of this report to search for a more detailed correlation between the two phenomena.

While the measurement techniques used to determine the irregularity region height and thickness appear to be consistent with previous studies, it is realized that an ad hoc independent check of these methods would be desirable. A check could be made using incoherent backscatter soundings, which give irregularity region height and thickness directly. With the accuracy established, the cross-correlation techniques described herein should be valuable for scintillation studies because of their relative simplicity and ease of application.

Bibliography

1. Basler, R. P. and DeWitt, R. N., "The Heights of Ionospheric Irregularities in the Auroral Zone," J. Geophys. Res., V. 67, 587-593 (1962).

2. Balsley, B. B., "Evidence of a Stratified Echoing Region at 150 Kilometers in the Vicinity of the Magnetic Equator during Daylight Hours," J. Geophys. Res., V. 69, 1925-1930 (1964).

3. Bolton, J. G., Slee, O. B., and Stanley, G. J., "Galactic Radiation at Radio Frequencies. VI. Low Altitude Scintillation of the Discrete Sources," Australian Journal of Physics, V. A6, 434-451 (1953).

4. Booker, H. G., "The Use of Radio Stars to Study Irregular Refraction of Radio Waves in Ionosphere," Proc. IRE, V. 46, 298-314 (1958).

5. Briggs, B. H., "A Study of the Ionospheric Irregularities which Cause Spread-F Echoes and Scintillation of Radio Stars," J. Atmos. Terr. Phys., V. 12, 34-45 (1958).

6. Briggs, B. H., Phillips, G. J., and Schinn, D. H., "Analysis of Fading at Spaced Receivers," Proc. Phys. Soc. London B, V. 63, 106-114 (1950).

7. Cohen, R. and Bowles, K. L., "On the Nature of Equatorial Spread-F," J. Geophys. Res., V. 66, 1081-1106 (1961).

8. Chivers, H. J. A., "The Location of the Irregularities Responsible for Ionospheric Scintillation of a Radio Source," Proc. of the International Conference on the Ionosphere (London), July, 1962, 258-266 (1963).

9. DeBarber, J. P., Chisholm, G. E., and Ross, W. J., "The Nature of the Irregularities in Ionization Density Causing Scintillations in Satellite Signals," Proc. of the International Conference on the Ionosphere (London), July, 1962, 267-270 (1963).

10. Dueno, B., "Study and Interpretation of Low Angle Fluctuations from the Radio Star Cassiopeia as Observed at Ithaca, N. Y.," Cornell Univ. School of Elect. Eng., Ithaca, N. Y., Tech Rep. No. 27, September 25, 1955.

11. Frihagen, J., and Trøim, J., "On the Large Scale Regions of Irregularities Producing Scintillation of Signals Transmitted from Earth Satellite," J. Atmos. Terr. Phys., V. 20, 215-216 (1961).

12. Hartridge, H., "The Scintillation of Stars," Nature, V. 165, 146-147 (1950).

13. Hewish, A., "The Diffraction of Galactic Radio Waves as a Method of Investigating the Irregular Structure of the Ionosphere," Proc. Roy. Soc. London A, V. 214, 494 (1952).

14. Hook, J. L., and Owren, Leif," The Vertical Distribution of E-Region Irregularities Deduced from Scintillations of Satellite Radio Signals," J. Geophys. Res., V. 67, 5353-5356 (1962).

15. James, P. W., "The Correlation Analysis of the Fading of Radio Signals Received from Satellites," J. Atmos. Terr. Phys., V. 24, 237-244 (1962).

16. Jespersen, J. L., and Kamas, George, "Satellite Scintillation Observations at Boulder, Colorado," NBS Report 7915, June, 1963. (To be published in J. Atmos. Terr. Phys.)

17. Hey, J. S., Parsons, S. J., and Phillips, J. W., "Fluctuations in Cosmic Radiation at Radio-Frequencies," Nature, V. 158, 234-238 (1946).

18. Kent, G. S., "High Frequency Fading Observed on the 40 mc/s Wave Radiated from Artificial Satellite 1957 α," J. Atmos. Terr. Phys., V. 16, 10-20 (1959).

19. Lawrence, Jr., J. D. and Martin, J. D., "Diurnal, Seasonal, Latitudinal, and Height Variations of Satellite Scintillation," J. Geophys. Res., V. 69, 1293-1300 (1964).

20. Lawrence, R. S., Jespersen, J. L., and Lamb, R. C., "Amplitude and Angular Scintillations of the Radio Source Cygnus-A," J. Research NBS, V. 65D, 333-350 (1961).

21. Liszka, L., "Satellite Scintillation Observed in the Auroral Zone," Arkiv for Geofysik, V. 4, 211-225 (1963a).

22. Liszka, L., "A Study of Ionospheric Irregularities Using Satellite Transmissions at 54 mc/s," Arkiv for Geofysik, V. 4, 227-246 (1963b).

23. Little, C. G., and Lovell, A. C. B., "Origin of the Fluctuations in the Intensity of Radio Waves from Galactic Sources," Nature, V. 165, 423-424 (1950).

24. Little, C. G., and Maxwell, A., "Scintillation of Radio Stars During Aurora and Magnetic Storms," J. Atmos. Terr. Phys., V. 2, 356-360 (1952).

25. Ludwig, G. H., and Whelpley, W. A., "Corpuscular Radiation Experiment of Satellite 1959 Iota (Explorer VII)," J. Geophys. Res., V. 65, 1119-1124 (1960).

26. McClure, J. P., "Polarization Measurements during Scintillation of Radio Signals from Satellites," J. Geophys. Res., V. 69, 1445-1447 (1964).

27. Megill, L. R. and Carleton, N. P., "Excitation by Local Electric Fields in the Aurora and Airglow," J. Geophys. Res., V. 69, 101-122 (1964).

28. Mendonca, F. de, Villard, Jr., O. G., and Garriott, O. K., "Some Characteristics of the Signal Received From 1958 δ 2," Proc. IRE, V. 48, 2028-2036 (1960).

29. Parthasarathy, R., Basler, R. P., and DeWitt, R. N., "A New Method for Studying the Auroral Ionosphere Using Earth Satellites," Proc. IRE, V. 47, 1660 (1959).

30. Roach, J. R., "Effects of Radio Wave Propagation Through Mid-Latitude 6300 A Auroral Arcs," J. Research NBS, V. 67D, 263-271 (1963).

31. Ryle, M. and Hewish, A., "The Effects of the Terrestrial Ionosphere on the Radio Waves from Discrete Sources in the Galaxy," Month. Not. Roy. Astronomical Soc., V. 110, 384-394 (1950).

32. Shimazaki, T., "A Statistical Study of World-Wide Occurrence Probability of Spread-F, Part 1, Average State, Part II Abnormal State in Severe Magnetic Storms," J. Radio Research Laboratories, V. 6, 669-704 (1959).

33. Smith, F. G., "Origin of Fluctuations in the Intensity of Radio Waves from Galactic Sources," Nature, V. 165, 422-423 (1950).

34. Spencer, M., "The Shape of Irregularities in the Upper Atmosphere," Proc. Phys. Soc., V. 68B, 493-503 (1955).

35. Swenson, Jr., G. W. and Yeh, K. C., "Summary of Satellite Scintillation Observations at the University of Illinois," Electrical Engineering Research Laboratory, University of Illinoia, Urbana, Illinois (August 4, 1961).

36. Warwick, James W., "Radio-Star Scintillations from Ionospheric Waves," J. Research NBS, V. 68D, 179-188 (1964).

37. Wild, J. P., and Roberts, J. A., "The Spectrum of Radio-Star Scintillations and the Nature of Irregularities in the Ionosphere," J. Atmos. Terr. Phys., V. 8, 55-75 (1956).

38. Yeh, K. C., "Propagation of Spherical Waves Through an Ionosphere Containing Anisotropic Irregularities," J. Research NBS, V. 66D, 621-636 (1962).

39. Yeh, K. C., Swenson, Jr., G. W., "The Scintillation of Radio Signals from Satellites," J. Geophys. Res., V. 64, 2281-2286 (1959).

40. Yeh, K. C. and Swenson, Jr., G. W., "F-Region Irregularities Studied by Scintillation of Signals from Satellites," J. Research NBS, V. 68D, (To be published in August, 1964).

41. Yeh, K. C., Swenson, Jr., G. W., and McClure, J. P., "A Phenomenological Study of Scintillation on Satellite Radio Signals," 1963 Spring URSI Meeting, Washington, D. C.

42. Yerukhimov, L. M., "Preliminary Results of Measurements of the Height of Ionospheric Inhomogeneities From Artificial Earth Satellite Signals," Geomagnetism and Aeronomy, V. 2, 572-574 (1962).